# 3D photonic integrated circuits for WDM applications

Ali Shakouri
Jack Baskin School of Engineering
University of California, Santa Cruz, CA 95064

Bin Liu, Patrick Abraham, John E. Bowers
Electrical and Computer Engineering
University of California, Santa Barbara, CA 93106

***Wavelength Division Multiplexing Critical Review, Optoelectronics '99***

**ABSTRACT**

The wafer fusion technique for realization of compact waveguide switches, filters and 3D photonic integrated circuits is investigated theoretically and experimentally. Calculations based on the beam propagation method show that very short vertical directional couplers with 40-220 μm coupling lengths and high extinction ratios from 20 to 32 dB can be realized. These extinction ratios can be further improved using a slight asymmetry in waveguide structure. The optical loss at the fused interface was investigated by comparison of the transmission loss in InGaAsP-based ridge-loaded waveguide structures with and without a fused layer near the core region. This reveals an excess loss of 1.1 dB/cm at 1.55 μm wavelength due to the fused interface. Fused straight vertical directional couplers have been fabricated and characterized. Waveguides separated by 0.6 μm gap layer exhibit a coupling length of 62 μm and a switching voltage of about 12 volts. Since GaAs and InP have different material dispersion at 1.55 μm wavelength, a combination of InP and GaAs couplers is used to demonstrate an inherent polarization independent and narrowband filter.

Keywords: Add/drop multiplexers, Integrated optoelectronics, Optical couplers, Optical filters, Optical switches, Optical waveguide components, Wafer bonding.

## 1. INTRODUCTION

A proliferation of various wavelength division multiplexing (WDM) components and systems in recent years has permitted rapid increases in fiber optics network capacity [1,2]. With the advent of Dense WDM (>80 wavelengths) and high-speed time division multiplexed (TDM) systems (>10 Gb/s), there is an increasing need for replacing slow and bulky conventional electronic routers and switches with photonic components. Optical waveguide devices and photonic integrated circuits provide a compact and low cost alternative for many network components. Various material properties (electro-optic, thermo-optic, acousto-optic etc.) in conjunction with active elements such as semiconductor optical amplifiers and lasers can be used to achieve different functionalities. Narrowband, polarization independent, low loss filters; low cross talk, scalable, high-speed photonic switches; and tunable add/drop multiplexers and

# Report Documentation Page

*Form Approved*
*OMB No. 0704-0188*



| 1. REPORT DATE | 2. REPORT TYPE | 3. DATES COVERED |
|---|---|---|
| **1998** | | **00-00-1998 to 00-00-1998** |

| 4. TITLE AND SUBTITLE | 5a. CONTRACT NUMBER |
|---|---|
| **3D photonic integrated circuits for WDM applications** | 5b. GRANT NUMBER |
| | 5c. PROGRAM ELEMENT NUMBER |
| 6. AUTHOR(S) | 5d. PROJECT NUMBER |
| | 5e. TASK NUMBER |
| | 5f. WORK UNIT NUMBER |
| 7. PERFORMING ORGANIZATION NAME(S) AND ADDRESS(ES) **Baskin School of Engineering,University of California,Santa Cruz,CA,95064** | 8. PERFORMING ORGANIZATION REPORT NUMBER |
| 9. SPONSORING/MONITORING AGENCY NAME(S) AND ADDRESS(ES) | 10. SPONSOR/MONITOR'S ACRONYM(S) |
| | 11. SPONSOR/MONITOR'S REPORT NUMBER(S) |

12. DISTRIBUTION/AVAILABILITY STATEMENT
**Approved for public release; distribution unlimited**

13. SUPPLEMENTARY NOTES
**The original document contains color images.**

14. ABSTRACT

15. SUBJECT TERMS

| 16. SECURITY CLASSIFICATION OF: | | | 17. LIMITATION OF ABSTRACT | 18. NUMBER OF PAGES | 19a. NAME OF RESPONSIBLE PERSON |
|---|---|---|---|---|---|
| a. REPORT | b. ABSTRACT | c. THIS PAGE | | | |
| **unclassified** | **unclassified** | **unclassified** | | **24** | |

demultiplexers are in the wish list of every photonic network operator. In this paper we describe a technique, wafer fusion, that can be used to overcome some of the shortcomings of the conventional *planar* photonic integrated circuits. This method allows for fabrication of three dimensional waveguide structures. In addition, materials with very different lattice parameters and physical properties can be combined to make novel devices with improved properties. In the following, we will first describe the wafer fusion technique for combining GaAs, InP and Si based devices. Beam propagation method (BPM) and coupled-mode theories are then used to study the theoretical performance of fused vertical waveguide couplers, i.e. their coupling length and extinction ratio. Experimental results for ultra short InP-based vertical couplers and switches are shown in Section 4. We will then describe the use of InP and GaAs fused waveguides to achieve polarization-independent narrow-band filters. The paper is concluded by a brief discussion of the future work and prospects for other WDM components.

# 2. WAFER FUSION

The technique of wafer fusion has been used to combine materials of very different lattice constants that could not be grown by heteroepitaxy [3,4]. Materials such as GaAs, InP and Si can be combined into a single device, without degrading the crystal quality away from the interfaces. Each section of a device can be optimized using the material best suited for its function. Examples are long wavelength vertical cavity surface emitting lasers with InGaAsP active region and GaAs/AlAs mirrors [5,6], or high gain-bandwidth product avalanche photodetectors with InGaAs absorption layer and Si multiplication region [7]. In this paper we will describe use of wafer fusion to fabricate three-dimensional photonic integrated circuits.

## *2.1. Semiconductor Wafer Fusion Technique*

Wafer fusion is a process in which two wafers are combined to form a single unit without the use of any intermediate layer such as epoxy or metal. Low electrical and thermal resistance and small optical loss at interface permits fabrication of active devices with fused layers inside. To achieve good fusion it is important that the two epitaxial surfaces are first cleaned and passivated such that there are minimum contaminants on the surface. Then the wafers are placed together in intimate contact under pressure (typically 2-3 MPa). Heating the wafers to near the growth temperature of one of the materials allows atomic redistribution to occur at the surface, filling in any deviation from the ideal, atomically smooth surfaces. After the wafers are cooled down, they should be strongly bonded. Ideally, the inherent crystal defects arising from the mismatch in lattice constants or surface states is localized exactly at the junction. In reality, wafer orientation and thermal mismatches may introduce other types of defects. A study of low temperature photoluminescence from quantum wells placed close to the fused InP/GaAs junction suggest that the material away from the fused interface (>100 nm) is of very high quality [3].

## *2.2. Optical Loss at Fused Interface*

Realization of 3D photonic integrated circuits requires a detailed optical characterization of the loss and uniformity of the fused interface. For this purpose, single mode waveguide structures were fabricated based on metal-organic chemical vapor phase deposited (MOCVD) material. The structure consisted of 0.5 μm InGaAsP ($\lambda_{gap}$=1.3 μm) guiding

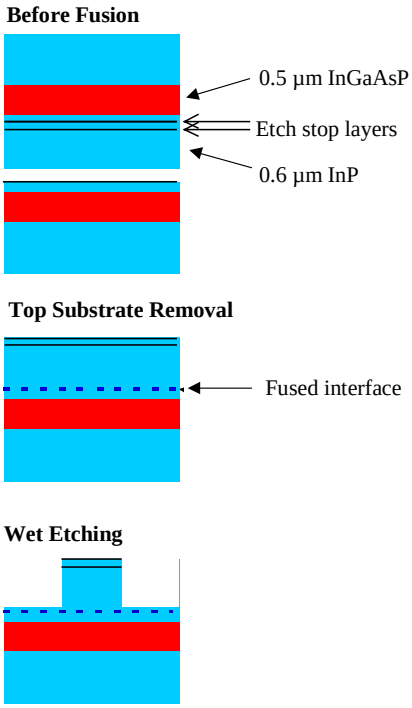


**Fig. 1 Different steps of fabrication process for single mode waveguide structure with a fused interface near core region.**

layer, 0.24 μm cladding layer which includes two 0.1 μm InP layers and two 0.02 μm InGaAsP ($\lambda_{gap}$=1.15 μm) etching stop layers, and finally 0.6 μm InP ridge layer. For the purpose of comparison, we use the same wafer and single mode waveguide geometry with and without a fused interface near the core region. The control waveguide has 3 μm wide and 0.6 μm high ridges defined using wet etching techniques. To fabricate the single mode fused waveguide, two 1×0.8 $cm^2$ samples are cut from the MOCVD grown wafer. First, the 0.6 μm InP layer and 0.1 μm cladding layer of one sample are removed using selective wet etching (Fig. 1); then 10 μm wide, 0.6 μm deep channels with 160 μm spacing are opened in a second sample. The two samples are then fused at 630$^{o}$C in a hydrogen atmosphere for 30 minutes. Subsequently, the InP substrate and 0.5 μm guiding layer of the top wafer are removed and 3 μm wide ridge waveguides are fabricated using wet etching. Fig. 2 shows a stain-etched SEM picture of finished device. The fused interface can not be seen in this picture. This is an indication of the high quality of the fused interface. The presence of the channels prior to fusion is crucial. Without these channels, we could see microscopic voids at the fused junction and many of the fabricated waveguides did not show clear eigenmodes.

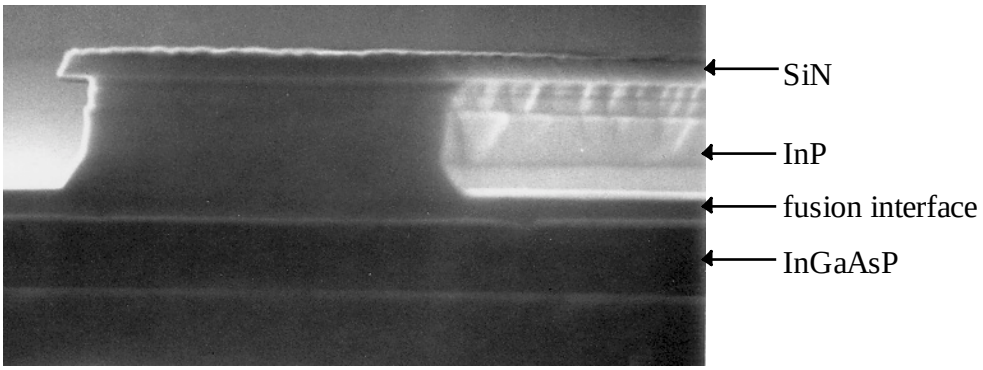


**Fig. 2 The stain etched SEM picture of the single mode waveguide structure with fused interface.**

The Fabry-Perot resonance technique was used to measure the optical propagation loss [8-11]. The optical loss of the unfused waveguide is about 2.4 dB/cm, while the fused structure showed a loss of 3.5 dB/cm at 1.55 μm. Since the geometry and materials are identical, the 1.1 dB/cm excess loss should be attributed to the fused interface. BPM calculations indicate that the field strength at the center of the fused interface is 49% of the maximum field. The issue of waveguide uniformity for large scale monolithic integration is very important. The size of our fused wafers is about $1\times0.8$ $cm^2$. After thinning and cleaving, the size of the sample for measurement is about $6\times6$ $mm^2$. The yield of the fused waveguides is more than 90% that is almost same as unfused sample. The existence of channels in fused sample provides 150 μm wide multimode slab waveguides that contain a fused interface. We did not notice any "dark" spots in these multimode structures.

We have also investigated mass transport at the fused interface by comparing samples with different effective fused areas. In conventional fused structures, after fabrication of narrow channels on one of the wafers prior to fusion, typically over 90% of the surface of the samples is in contact during the fusion process. We studied samples where the fusion was only over the surface on the top of waveguides (3 to 6 microns thickness, separated by 125 microns, and about 1cm long). In this case only 4% of the surface of the two wafers is in contact during fusion. We did not notice any substantial degradation or nonuniformity in the ridge waveguide structure.

# 3. VERTICAL COUPLERS

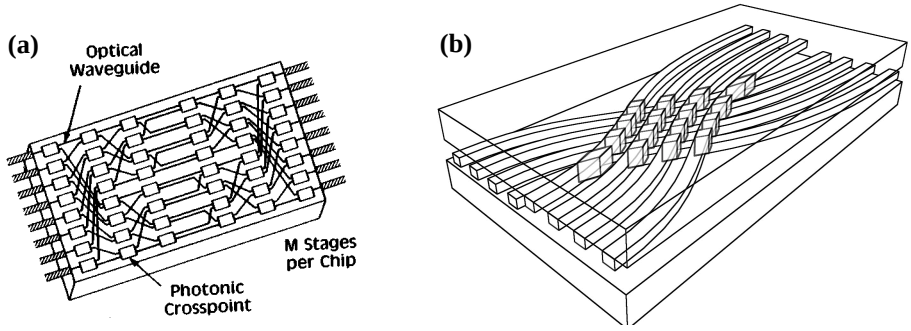


**Figure 3 (a) A conventional planar photonic integrated circuit. (b) 3D structures based on wafer fusion and coupling between independent arrays of waveguides on different substrate.**

## *3.1. Multiple Level Interconnects*

Conventional photonic integrated circuits rely upon a single plane of interconnect (Fig. 3a). Multiple layers of interconnection were developed in early days of electronic integrated circuits as the circuit complexity increased. This development has not occurred in photonics because the different layers have to be crystalline, and crystalline deposition of low loss waveguides after patterning is difficult with epitaxy and impossible by sputtering or evaporation (as is done in electronics). Combining planarized dielectric waveguides with polymer or glass waveguides is an option. One has to match the indices using grating or ARROW structures, and in addition one loses many advantages of active amplifiers and other optical properties of semiconductors. We will see in the following that wafer fusion can be used to combine planar waveguides fabricated on two different substrates into a three-dimensional structure in which there is vertical coupling between arrays of single mode waveguides (Fig. 3b).

| | Wavelength (μm) | Operating Voltage (V) | Extinction Ratio (dB) | Coupling Length (μm) |
|---|---|---|---|---|
| **K. Tada et al.**[12] Univ. of Tokyo (1974) | 1.15 | 10 | no | no |
| **M. Cada et al.**[13] Nova Scotia, Canada (1989) | 0.85 | 1 V/cm | no | 160 |
| **J. Cavaillès et al.**[14] Philips, France (1989) | 0.88 | 5 | no | 90-110 |
| **M. Kohtoku et al.**[15] Tokyo Inst. Tech. (1991) | 1.57 | 20 | no | 170 |
| **F. Dollinger et al.**[16] Munich, Germany (1996) | 0.854 | 5 | > 10 | 85 |
| **B. Boche et al.**[17] Munich, Germany (1996) | 0.86 | 4 | > 16 | no |
| **B. Liu et al.**[11] UCSB, US (1998) | 1.55 | 12 (2.8) | ~ 15 | 62 |
| **S. Ikuta et al.**[18] Yokohama, Japan (1998) | 1.55 | - | | 350 |

**Table 1 Some examples of waveguide vertical couplers and switches.**

Despite the practical difficulty of separating the two input or output waveguides in conventional high mesa vertical directional couplers, they have been studied by various research groups [12-20] (see table 1). In fact vertical couplers are attractive candidates to realize photonic switches and narrow band filters because of their very short coupling length and feasibility of integration with other optoelectronic devices. In the following we will analyze the theoretical performance of the fused vertical and conventional planar directional couplers.

## *3.2. Beam Propagation Method Analysis*

In order to calculate the coupling length and the extinction ratio in 2D fused waveguide structures a 3D finite difference beam propagation program is used [21]. The fused vertical coupler (FVC) is shown in Fig. 4. A single-mode ridge-loaded waveguide structure based on InP substrate, with 0.5 μm InGaAsP ($\lambda_{gap}$ =1.3 μm) core region, 0.1 μm cladding and 0.1 μm ridge height, is vertically coupled through a fused gap layer to an identical waveguide. The gap layer thickness is varied from 0.1 to 0.6 micron with its index ranging from InP to InGaAsP ($\lambda_{gap}$=1.4 μm) [48-49].

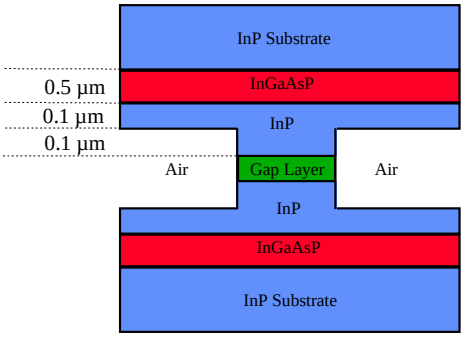


**Fig. 4 The coupling region between two fused waveguides.**

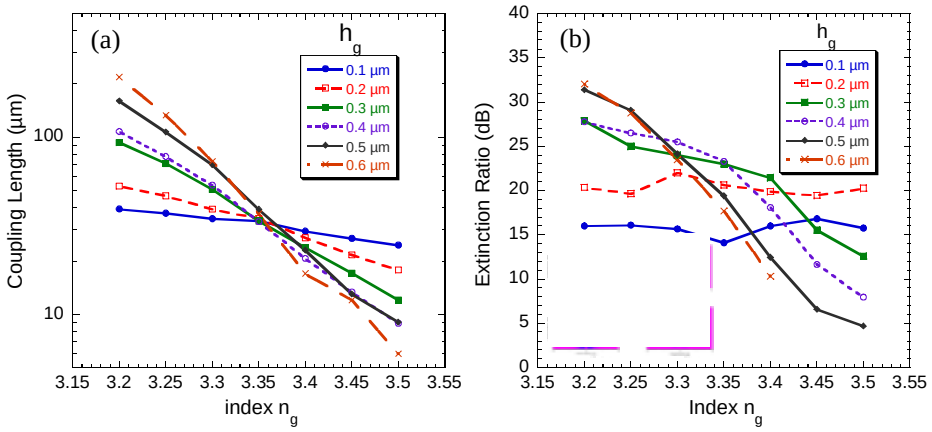


**Fig. 5 The coupling length (a) and the extinction ratio (b) as a function of gap layer index for different thicknesses of the gap layer(λ=1.55 µm).**

Fig. 5(a) displays the coupling length for different parameters of the gap layer. As expected, increasing the gap layer index reduces the coupling length. In a coupled-mode picture, this can be explained by an increase in the overlap integral of the two modes of adjacent waveguides. On the other hand, the dependence of the coupling length on the gap layer thickness shows a mixed behavior. When the gap region has small indices close to InP layer, increasing its thickness will decouple the two waveguides and thus increases the coupling length (see Fig 7a). However, when the index of the gap layer is large (close to 1.3 µm quartenary), the mode amplitude in this region is not anymore exponentially decaying, but sinusoidal. So a thicker gap layer will increase the overlap integral between modes of adjacent waveguides and thus reduces the coupling length (see Fig. 7b). When the gap layer thickness is more than 0.3-0.4 µm, an analysis based on the supermodes of three coupled waveguide is more appropriate, but the appearance of undesirable modes in the gap layer will deteriorate the performance of the directional coupler.

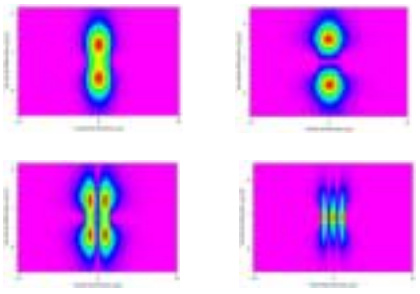

**Fig. 6 Supermodes of fused vertical coupler for $h_{gap}$= 0.4 µm and $n_{gap}$=3.4.**

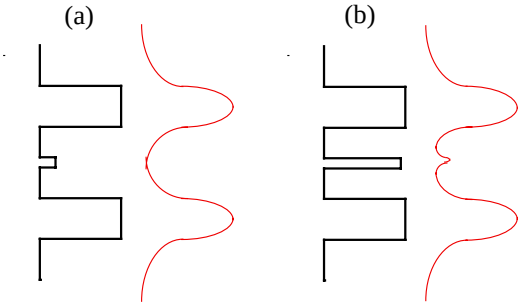


**Fig. 7 Cross section index and field profiles for the vertical coupler with low-index gap region (a) and high-index gap region (b).**

In order to quantify the effect of higher order modes, power transfer between two waveguides was analyzed. The eigenmode of one of the uncoupled waveguides was taken for the input field, and power transfer to the other waveguide as a function of propagation distance was monitored by BPM simulation. Fig. 5(b) displays the extinction ratio defined as the ratio of mode powers in the two waveguides after a coupling length. When the gap layer thickness and its index are high, the coupler has poor extinction ratios of 5 to 10 dB. In this case BPM simulation reveals 3 to 4 supermodes in the coupling region (see Fig. 6). In additional to the expected symmetric and antisymmetric eigenmodes, there are modes of the gap layer and some leaky modes. But for a wide range of parameters (gap thickness from 0.2 to 0.6 μm, and gap index from 3.2 to 3.4), extinction ratios of 20 to 32 dB can be achieved. From Fig. 5(a) we see that this corresponds to coupling lengths of the order of 40 to 220 microns. Since the two waveguides are very close, it is almost impossible to excite only one of them and to measure the extinction ratio experimentally. In practice, the two ridge structures will be separated by curved regions and the on/off ratio is limited by unwanted coupling at regions where the waveguides join together and non ideal fabrication process. The above analysis, however, shows the inherent limitation in extinction ratios.

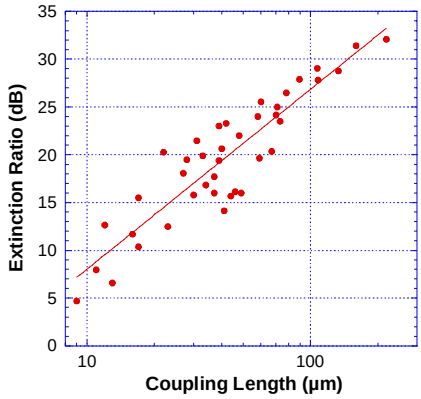


**Fig. 8 Extinction ratio as a function of coupling length for the data in Fig. 5.**

In these symmetric ultra short couplers, the main problem to achieve low extinction ratio is non-orthogonality of the modes of individual waveguides [22-27]. As the coupling length decreases, the overlap integral between individual waveguide modes increases and subsequently the extinction ratio deteriorates (see Fig. 8). It is interesting to note that the extinction ratio ($P_{on}/P_{off}$) is approximately proportional to the square of the coupling length (i.e. $10\log(P_{on}/P_{off}) \propto 20 \log(\text{coupling length})$). Using a slight asymmetry, one can improve extinction ratios to arbitrary small values. An intuitive picture is that a slight asymmetry can equalize the overlap integral of the single waveguide mode with the symmetric and antisymmetric supermodes of the coupler and thus increase the extinction ratio [28-29]. Another method to eliminate the crosstalk problems for ultra short couplers is the use of tapering at input and output regions [30].

### 3.3. *Polarization and Wavelength Sensitivity*

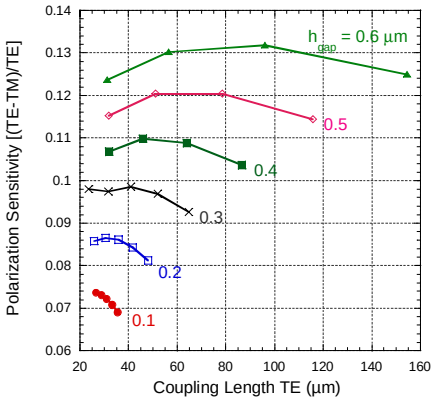


**Fig. 9 Polarization sensitivity for various waveguide parameters in Fig. 5.**

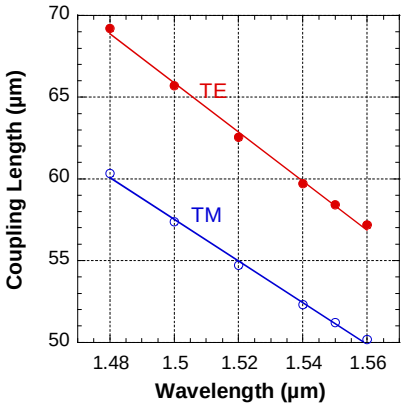


**Fig. 10 Wavelength dependence of the coupling length for 0.2 μm thick InP gap layer.**

An important requirement for optical switches is polarization insensitivity. The fused vertical coupler shown in Fig. 4 has coupling length for TM polarized light at 1.55 μm wavelength which is 7 to 13% shorter than the TE one. Fig. 9 displays the polarization sensitivity (i.e. the ratio of coupling lengths (TE-TM)/TE) calculated using improved coupled mode theories [28,29,33]. It can be seen that thin gap layers are less polarization sensitive than the thick ones. We will see in the following that it is possible to make the switch polarization insensitive using the difference in materials dispersion e.g. by combining GaAs and InP waveguides [31].

For many WDM applications, such as add/drop multiplexers and demultiplexers, one has to study the wavelength dependence of the coupling length. Fig. 10 shows this dependence for TE and TM polarizations for a 0.2 μm thick InP gap layer. A change of operating wavelength by 80 nm, modifies the coupling length by ~20%. Thus, a symmetric vertical coupler of 2.4 mm total length can demultiplexe two WDM channels separated by 1nm. Methods used to produce flat-top response in planar structures by making multi section coupling regions can also be used in these vertical couplers.

Vertical coupling through the ridge structure whose height is defined by etch-stopping techniques is much less sensitive to the ridge waveguide width and sidewall smoothness than the planar waveguide couplers. In fact, the difficulty in making reproducibly and uniformly very narrow gap (<1 μm) couplers have mitigated their development for ultra short switching devices. Fig. 11(a) shows the coupling length as a function of waveguide width for the case of a conventional ridge-loaded structure with 0.5 μm InGaAsP ($\lambda_{gap}$= 1.3 μm) core layer, 0.1 μm InP slab layer and 0.2-0.4 μm InP ridge. The centers of the two waveguides are separated by 4-6 μm. It can be seen that a change of 1 μm in

waveguide width will change the coupling length by 20 to 40%. When the same waveguides are coupled vertically (Fig. 11(b)), the coupling length is about 1-2 orders of magnitude smaller and at the same time less sensitive to waveguide width variation (4 to 5% change in coupling length for one micron change in waveguide width).

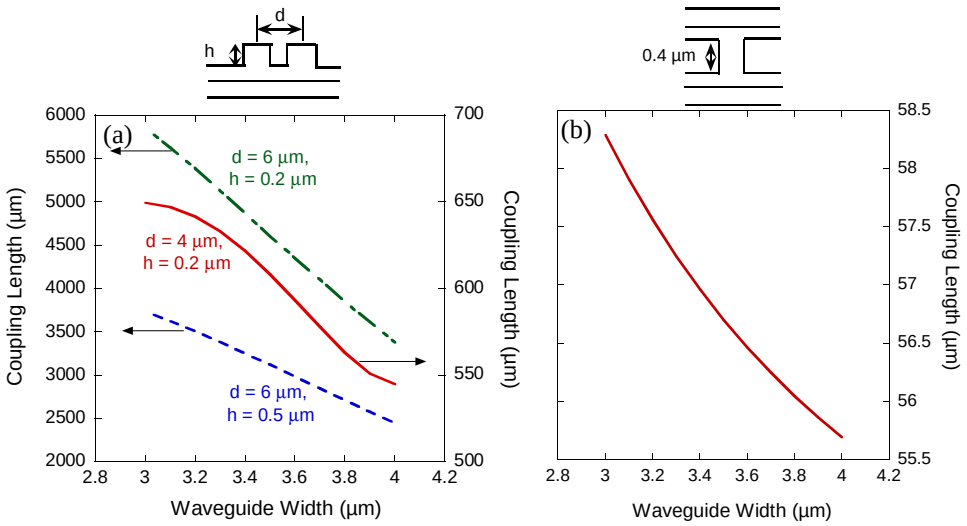


**Fig. 11 The waveguide width dependence of the coupling length for a conventional planar coupler (a) and a vertical coupler (b).**

# 4.FUSED WAVEGUDIES

Having discussed the theoretical advantages of vertical couplers and the flexibility that wafer fusion offers to realize such devices, in this section we will look at some experimental results for ultrashort fused vertical couplers and switches.

## *4.1. Fused Vertical Coupler*

The structure of the coupler is identical to that in Fig. 4, with 0.2 μm thick InP gap layer. The material was grown by MOCVD and consisted of a 0.5 μm InGaAsP ($\lambda_{gap}$=1.3 μm) guiding layer on InP substrate, followed by 0.1 μm InP cladding layer, 20 nm InGaAsP ($\lambda_{gap}$=1.15 μm) etch stop layer and 0.4 μm InP coupling layer. To fabricate the vertical coupler, two 8×10 $mm^2$ samples are cleaved from the grown wafer. In the first sample the top 0.4 μm InP layer is removed. On the second sample, a ridge waveguide structure is fabricated using standard photolithography and selective wet etching. The ridges have 3-6 μm width, 0.4 μm height and they are separated by 125 μm. The two samples are then fused together at a temperature of 630$^{o}$C in a hydrogen atmosphere for 30 minutes. Fig.12(a) shows the stain etched SEM picture of a finished fused vertical coupler (FVC). The fused interface is not visible, even after staining. There is mass transport at the edge of the ridge. This is beneficial to get a symmetric coupler and improves the side wall flatness.

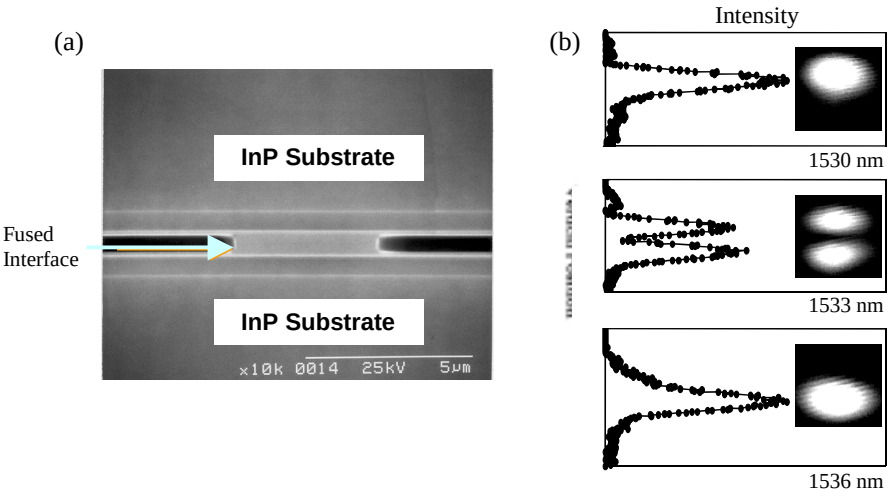


**Figure 12 (a) The stained etched SEM picture of a fused vertical coupler. (b) Photograph of the near field pattern at 1530, 1533 and 1536 nm. The width of the ridge is 3 µm, and the distance between upper and lower waveguides is 1.1 µm.**

The near field pattern at the output of FVCs, 5.5 mm long, is recorded by an IR camera and is shown in Fig. 12(b). The light is input from an 8 µm diameter single mode 1.55 µm fiber. It can be seen that by changing the input wavelength, light is switched from the upper to the lower waveguide. Fig. 13 shows the intensities of the upper and lower waveguides as a function of wavelength. Our measurements show that the extinction ratio can be > 15dB. This is particularly difficult to achieve in conventional high mesa vertical couplers [12-18]. From the oscillation period (about 12nm) and considering material and waveguide dispersions, the index difference between the even and odd modes can be calculated which is 0.0121. The corresponding coupling length is 62 µm at 1.55 µm that agrees very well with 58 µm result from BPM simulations.

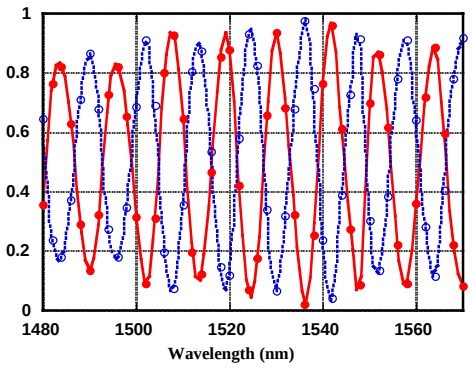


**Fig. 13 Measured intensity of the upper (closed circle) and lower (open circle) waveguides as a function of wavelength.**

## 4.2. *Fused Vertical Switch*

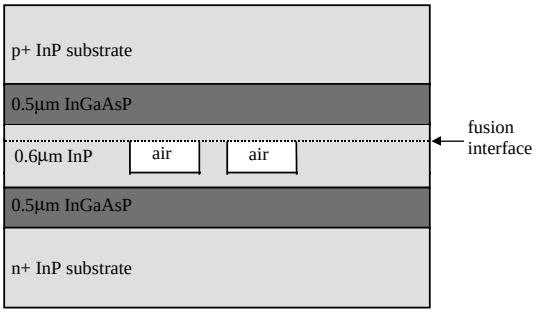


**Fig. 14 Schematic drawing of a fused vertical coupler switch.**

The structure of the PIN fused vertical coupler is identical to the one in Fig. 12(a), the only difference is that the top InP substrate is p-doped and the bottom wafer n-doped. To support the narrow, 2 μm to 5 μm wide, 0.4 μm high ridges during the fusion process, 10 μm wide InP layers were etched on both sides of the ridges as shown in Fig. 14. The adjacent ridge waveguides are separated by 125 μm. After fusion, the sample was thinned to 200 μm using an HCl etchant. Then 300 nm gold was deposited on both sides for applying the bias voltage.

Fig. 15 (a) shows the measured I-V curves of FVCs. The sample size is 3.5×4.5 $mm^2$. Since 80% of the area of two samples are fused together, and only 3% of this area are the

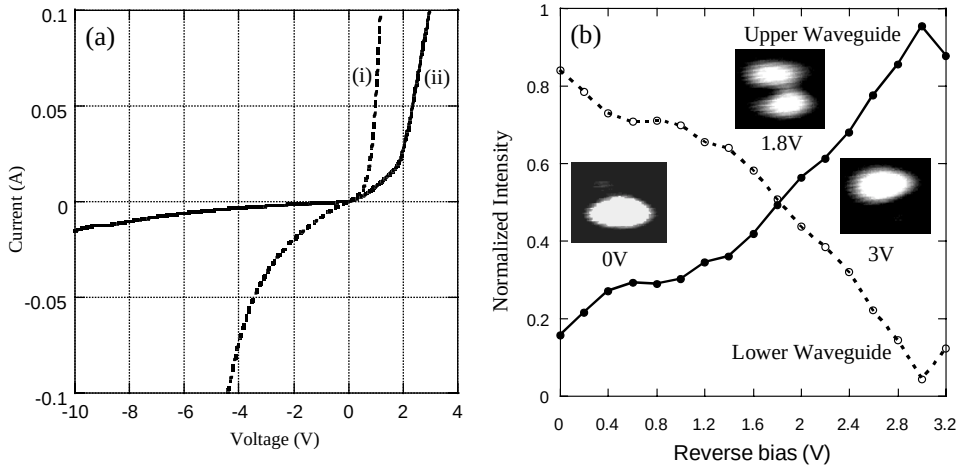


**Fig. 15 (a) I-V curves of PIN-FVC with broad (i) and narrow (ii) ohmic contacts. (b) Measured intensity of the upper (closed circle) and lower (open circle) waveguides as a function of reverse bias for a broad area ohmic contact FVC.**

actual ridge waveguide, there is a large leakage current that can be reduced by etching mesas and depositing metal only on the FVC ridge regions. When wafer fusion technique is used to fabricate VCSELs and detectors [3,5-7], those devices are relatively small and uniformity of the fused material is not so critical for individual device operation. To make long waveguide couplers and switches, on the other hand, requires a good uniformity of the fusion interface. We used electroluminescence images of FVC to study the fusion uniformity under current flow. The near field pattern at the output facet of the coupler was observed by an IR camera. The luminescence image of a 64 μm wide fused area at 200 mA forward current did not show any dark regions and the intensity was very uniform along the fused interface [32].

To characterize FVCs, a tunable laser is used to launch light at the input of the coupler through an 8 μm diameter single mode fiber. The near field images at the output of a 3.5 mm long FVC for three reverse biases 0V, 1.8V and 3V are shown in Figure 15(b), along with the normalized intensities of upper and lower waveguides. The linear electrooptic effect at 3V is too small to explain the switching. We believe that the thermo-optic effect plays a major role in this device because of the high leakage current that contributes to internal heating of this structure. To conform this, we changed the stage temperature, and switching is observed when 30°C temperature change. In order to reduce the leakage current, we fabricated another FVC. In this case, one of the InP substrates is removed and the electrodes are evaporated on the exact ridge area through narrow windows of a SiN insulation layer. The I-V curve of a 7mm×3 μm FVC with this modification is shown in Fig. 15 (a) (curve (ii)). As it can be seen in Fig. 16, a 12V reverse bias is needed to achieve switching. The insert pictures show the near fields at different biases. Using quantum well structures, the switching voltage can be further reduced.

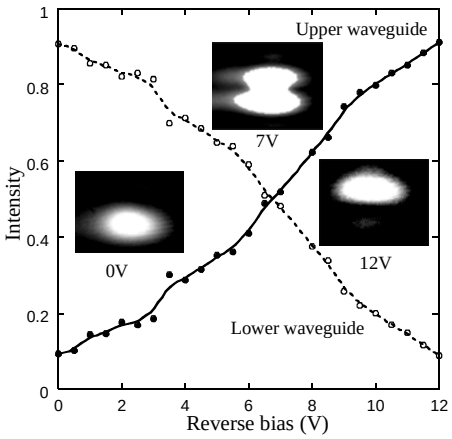


**Fig. 16 Measured intensity of the upper (closed circle) and lower (open circle) waveguides as a function of reverse bias for a narrow area ohmic contact FVC.**

## 4.3. Asymmetric Fused Vertical Directional Coupler

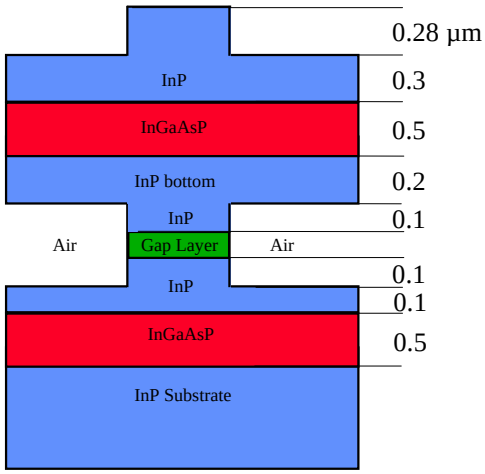


**Fig. 17 Asymmetric fused vertical coupler**

In order to fabricate multi level 3D photonic integrated circuits, an asymmetric fused structure is needed (see Fig. 17). By repeating the fusion process, one can obtain multiple layers of waveguide interconnects. For fabrication, first, a set of ridge waveguides on an InP wafer is defined using the usual wet and dry etching techniques. Subsequently, a wafer is bonded on top of the waveguides. After removing the substrate of this top wafer using selective etching, a second set of waveguides is fabricated. These top waveguides are coupled vertically to the waveguides beneath them in areas where the two structures are connected by wafer fusion. The issue of alignment in the coupling regions is facilitated using infrared photolithography.

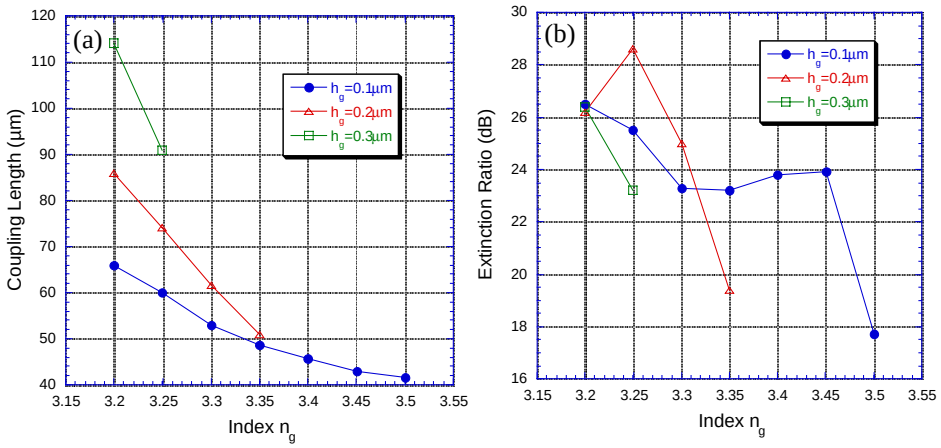


**Fig. 18 The coupling length (a) and the extinction ratio (b) as a function of gap layer index for different thicknesses of the gap layer, for asymmetric fused vertical coupler.**

Even though the top and bottom waveguides are very dissimilar, by matching the mode effective indices, one can theoretically achieve coupling lengths of the order of 60 microns with 25 dB extinction ratio (see Figs. 18 (a) and (b)). Fig. 19 displays the SEM cross section of the bottom and top waveguides along with the near field infrared image at the output of an InGaAsP asymmetric coupler where the two waveguides are separated by 250 μm.

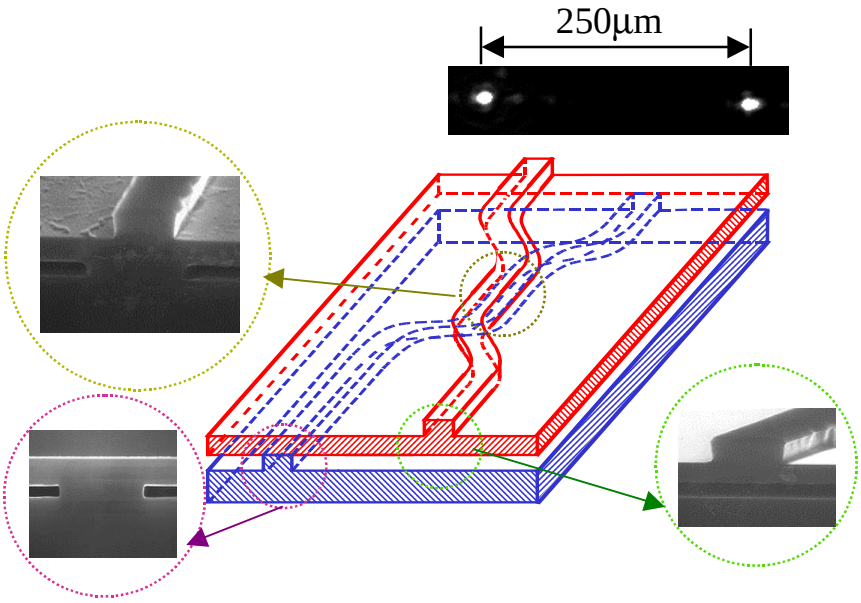


**Fig. 19 SEM pictures of the separated top and bottom waveguides for an asymmetric fused vertical coupler. The bottom picture is a photograph of the near field pattern at the output of the coupler where the two waveguides are separated by 250 μm.**

## 5.InP/GaAs FUSED FILTER

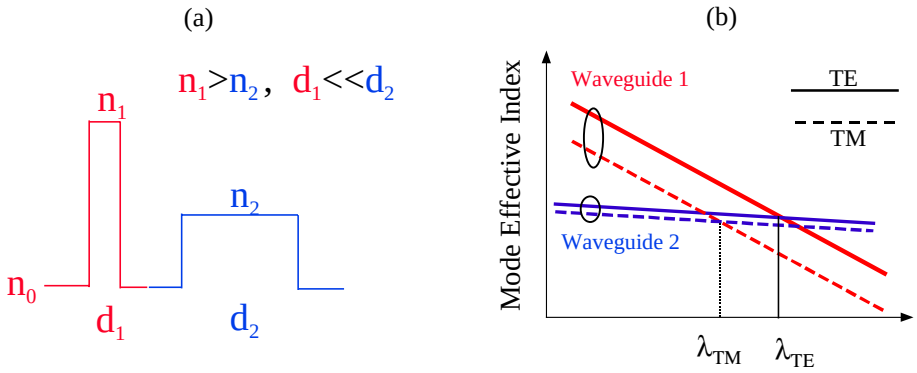


**Fig. 20 (a) Index profile for conventional asymmetric vertical coupler. (b) The corresponding modal effective index as a function of wavelength. $\lambda_{TE}$ ($\lambda_{TM}$) is the filter resonance wavelength for TE (TM) polarized light.**

Integrated compact and narrowband optical filters are key components for dense WDM systems. Asymmetric vertical directional coupler filters [36-47] using two dissimilar waveguides on III-V semiconductors are promising because of the precise control of waveguide thickness and indices and monolithic integration with other devices. It is well known that the linewidth of the asymmetric directional coupler is inversely proportional to both the device length and the difference of mode dispersion in the two waveguides. To minimize the device length and reduce the sidelobes, the filter bandwidth can only be narrowed by increasing the mode dispersion difference. The modal dispersion depends on two factors. One is waveguide dispersion that depends on waveguide geometry; the other one is the material dispersion. Vertical coupler filters realized up to now use mainly the waveguide dispersion difference. A narrow bandwidth filter requires one of the waveguides to have a very small index difference between the core and the cladding, and a large core size, while the other one should have a large index difference and a small core size (see Fig. 20).

To keep single mode operation and a high fiber coupling efficiency, the waveguide core size can not be too large or too small, and this limits the bandwidth of the filter. Very dissimilar waveguide structures have also strong polarization dependence that is a disadvantage in fiber communication systems. Another major obstacle to apply conventional vertical coupler filter to WDM systems is how to launch light into and couple out of two very close waveguides.

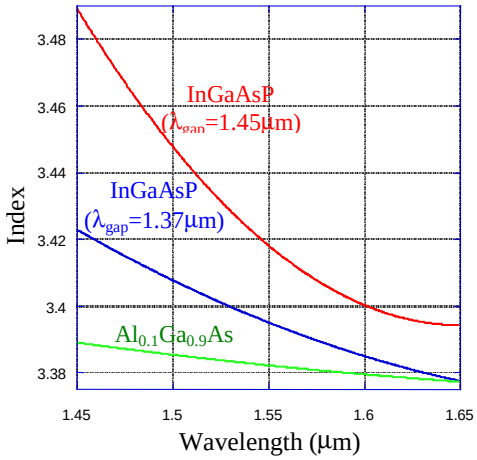


**Fig. 21 Material dispersion for $In_{0.65}Ga_{0.35}As_{0.8}P_{0.2}$ ($\lambda_{gap}$=1.45μm), $In_{0.67}Ga_{0.33}As_{0.7}P_{0.3}$ ($\lambda_{gap}$=1.37μm), and $Al_{0.1}Ga_{0.9}As$.**

Fused vertical couplers, on the other hand, can combine different material systems. GaAs/AlGaAs has a low material dispersion at 1.55μm, while InP/InGaAsP has large material dispersion (see Fig. 21). With a proper design, a very narrowband and polarization independent monolithic filter with separated inputs and outputs can be realized.

The structure of the proposed fused vertical coupler filter is illustrated in Fig. 22(a). The upper InGaAsP/InP waveguide consists of 0.4 μm InGaAsP ($\lambda_{gap}$=1.45μm) guiding layer, and InP cladding layer. The lower AlGaAs/GaAs waveguide includes 0.53μm $Al_{0.1}Ga_{0.9}As$ core and 0.2 μm $Al_{0.5}Ga_{0.5}As$ cladding layers. These two waveguides are phase matched at 1.55 μm. The material dispersion of InGaAsP ($\lambda_{gap}$=1.45μm) is –0.48 /μm at 1.5μm which is almost one order higher than the material dispersion of

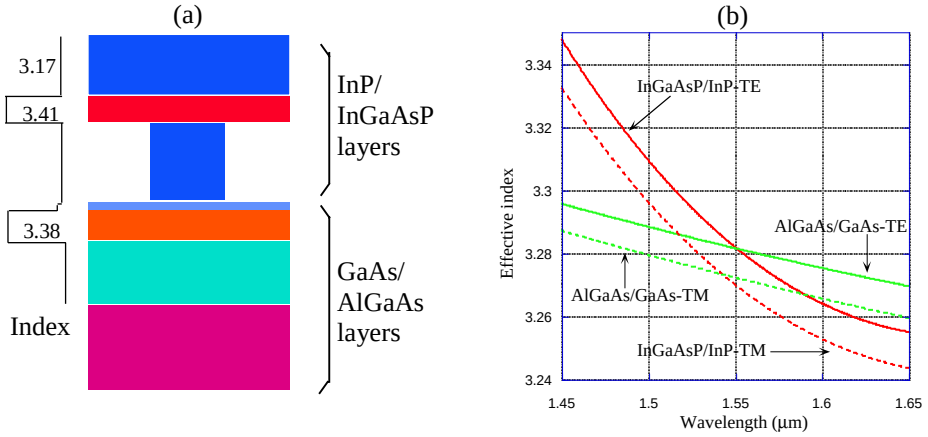


**Fig. 22 (a) The structure of InP/GaAs fused vertical coupler filter and (b) the calculated modal dispersion for the two waveguides for TE and TM polarizations.**

$Al_{0.1}Ga_{0.9}As$ –0.059 /μm. Fig. 22(b) shows the calculated modal dispersion of upper and lower waveguides. Most of the wavelength dependence comes from material's contribution. In conventional structures, the polarization dependent wavelength shift is about 30-40nm. In the current structure because of similar waveguide geometry and dimensions, there is only 8 nm polarization dependent wavelength shift. By replacing the $\lambda_{gap}$=1.45 μm InGaAsP quartenary with 1.37 μm one, the filter becomes polarization independent. Since the material dispersion of 1.37 μm quartenary is little lower than that of 1.45μm quartenary, a small bandwidth will be sacrificed in this structure.

Using 3D beam propagation method (BPM), the performance of fused filters is simulated. When the separations of two waveguides $d_s$=1.2μm, 1.6μm and 2μm, the corresponding coupling lengths (100% power transfer) are 1mm, 4.5mm and 2cm and the bandwidths are 4nm, 0.8nm and 0.2nm at the coupling length. As we expected, the central wavelength is independent of the separation distance of two waveguides and the bandwidth is inversely proportional to the coupler length. Because of uniform coupling, there is a -9dB side lobe, which is too high for practical application. This can be resolved by using X-crossing structures [42-44]. Fig. 23 displays coupling coefficient as a function of propagation distance for X-crossing fused vertical coupler. The "gradual" coupling in real space will result in better side-lobe suppression in frequency domain. Fig. 24 shows the calculated response of the X-crossing structure with an angle $\theta$=0.16° using coupled mode theory. One can see that the side lobe is suppressed to more than -40dB, which is sufficient for the requirement of most WDM systems. One should note that the fabrication of X-crossing vertical coupler filter structure with separated inputs and outputs is very easy with the use of wafer fusion technology.

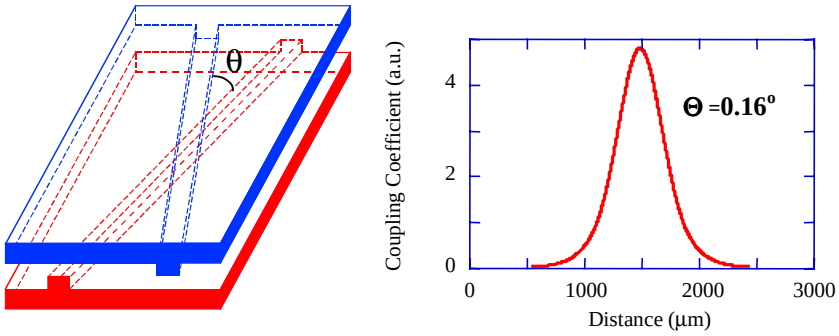


**Fig. 23 Coupling coefficient as a function of propagation distance for X-crossing fused vertical coupler filter with θ = 0.16°. The separation between top and bottom wafers (i.e. total ridge height) is 1.2 μm.**

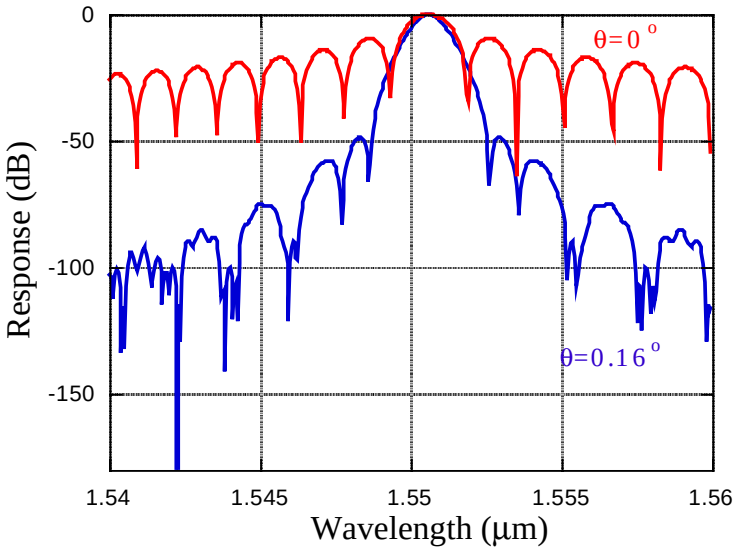


**Fig.24 The response of an X-crossing fused vertical coupler filter with θ=0° and 0.16°. Vertical separation of the waveguides is 1.2μm.**

We have fabricated a fused straight (θ=0°) vertical coupler filter based on MBE grown GaAs and MOCVD grown InP waveguides. The structure is shown in Figs. 22(a) and 25. The separation of two waveguides is 1.2 μm, which corresponds to 1mm coupling length. A 1 mm long device has been measured. Fig. 26(a) shows the measured response, the 3dB bandwidth is 3.6 nm, which agrees well with theoretical value of 3.9 nm. The measured coupling efficiency (the optical power from the output waveguide divided by the sum of the optical power from both the output and input waveguides) of the current device is about 50%. The polarization dependent wavelength shift is only 5 nm. Theoretical calculations predict a 7nm shift. This polarization dependence can be eliminated with a proper design. To optimize the design of fused InP/GaAs coupler, one should take into account material losses. The bandgap of InGaAsP guiding layer is closer than GaAs/AlGaAs material to the operation wavelength at 1.55μm. One thus expects

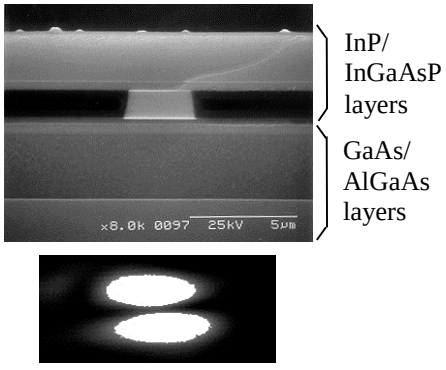


**Fig. 25 The stained etched SEM picture of InP/GaAs fused vertical coupler filter. The bottom curve shows a photograph of the near field pattern at the output. Note the similar mode shapes of the top and bottom waveguides.**

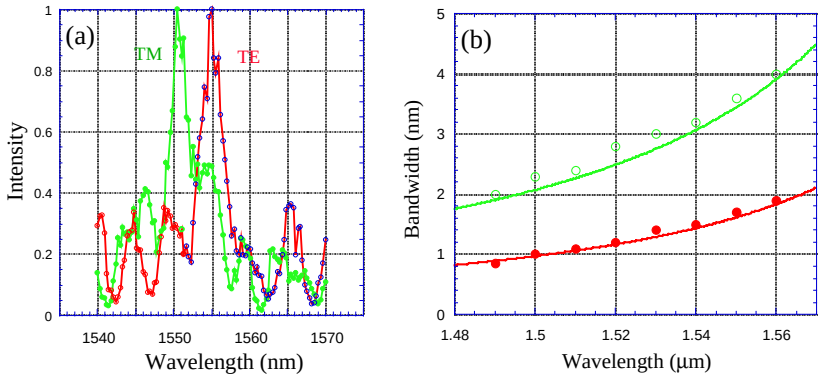


**Fig. 26 (a) The measured response of a 5 μm wide fused vertical coupler for TE and TM polarizations. (b) Experimental (circles and squares) and theoretical (lines) wavelength dependence of the bandwidth for a 3 mm long fused filter.**

larger band-to-band absorption in InGaAsP waveguides. However in doped materials, free carrier absorption increases and dominates when the wavelength is farther from the bandgap. We have measured 4-6dB/cm optical propagation loss for both InP/InGaAsP and GaAs/AlGaAs waveguides at 1.55μm. We did not notice a substantial increase in loss for the lower bandgap material InGaAsP. The fusion process adds 1-3dB/cm loss [11].

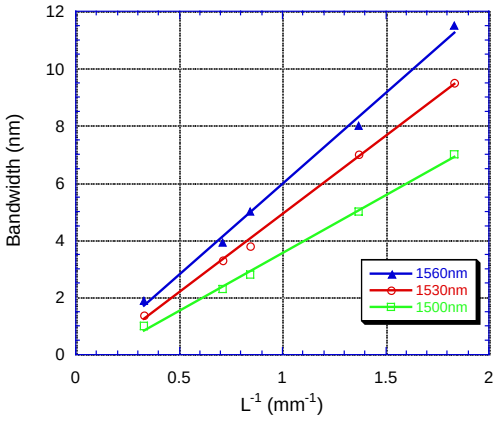


**Fig. 27 Experimental (points) and theoretical (lines) coupler length dependence of the bandwidth.**

## 6. SUMMARY AND CONCLUSION

In conclusion, wafer fusion technique for fabrication of vertical couplers and switches is described. Very short directional couplers with a coupling length of 40-220 microns and high extinction ratios of 20 to 32 dB can be realized. These extinction ratios can be further increased using a slight asymmetry in waveguide structure or with tapering the input and output regions. It is shown that 1.1 dB/cm excess optical loss is introduced due

to fusion process in InP based waveguides at 1.55 μm wavelength. Fused straight vertical directional couplers separated by 0.6 μm gap layer exhibit a coupling length of 62 μm and a switching voltage of about 12 volts. These fused waveguides give us the added advantage of vertical dimension by separating the input and output waveguides to realize compact and scalable 3D photonic integrated circuits.

This technology can be extended to a whole family of devices, from couplers and switches to filters and tunable lasers. Additional levels of interconnect can be demonstrated, allowing additional complexity to future photonic integrated circuits.

## ACKNOWLEDGEMENTS

This work is supported by the AFOSR and DARPA center MOST.

## REFERENCES

1. Chraplyvy, A. R., and R. W. Tkach, "Terabit/second transmission experiments," IEEE J. Quantum Electron., vol. 34, pp. 2103-2108, November 1998.
2. Kawanishi, S., "Ultrahigh-speed optical time-division-multiplexed transmission technology based on optical signal processing," IEEE J. Quantum Electron., vol. 34, pp. 2164-2179, November 1998.
3. Black, A., A. R. Hawkins, N. M. Margalit, D. I. Babic, A. L. Holmes, Y.-L. Chang, P. Abraham, J. E. Bowers, E. L. Hu, "Wafer fusion: materials issues and device results," IEEE J. Select. Topics Quantum Electron., vol. 3, pp. 943-51, June 1997.
4. Zhu, Z.-H.; Ejeckam, F.E.; Qian, Y.; Jizhi Zhang; and others, “Wafer bonding technology and its applications in optoelectronic devices and materials,” IEEE Journal of Selected Topics in Quantum Electronics, June 1997, vol.3, (no.3):927-36.
5. Babic, D.I.; Streubel, K.; Mirin, R.P.; Margalit, N.M.; and others, “Room-temperature continuous-wave operation of 1.54- mu m vertical-cavity lasers,” IEEE Photonics Technology Letters, Nov. 1995, vol.7, (no.11):1225-7.
6. Margalit, N.M.; Zhang, S.Z.; Bowers, J.E., “Vertical cavity lasers for telecom applications,” IEEE Communications Magazine, May 1997, vol.35, (no.5):164-70.
7. Hawkins, A.R.; Weishu Wu; Abraham, P.; Streubel, K.; and others, “High gain-bandwidth-product silicon heterointerface photodetector,” Applied Physics Letters, 20 Jan. 1997, vol.70, (no.3):303-5.
8. Walker, R.G., “Simple and accurate loss measurement technique for semiconductor optical waveguides,” Electronics Letters, 20 June 1985, vol.21, (no.13):581-3. And also Erratum: Electronics Letters, 1 August 1985, vol.21, (no.16):714.
9. Park, K.H.; Kim, M.W.; Byun, Y.T.; Woo, D.; and others, “Nondestructive propagation loss and facet reflectance measurements of GaAs/AlGaAs strip-loaded waveguides” Journal of Applied Physics, 15 Nov. 1995, vol.78, (no.10):6318-20.
10. Ching-Ting Lee, “Nondestructive measurement of separated propagation loss for multimode waveguides,” Applied Physics Lett., 13 July 1998, vol.73, (no.2):133-5.
11. Liu, B., A. Shakouri, P. Abraham, B. -G. Kim, A. W. Jackson, and J. E. Bowers, "Fused vertical couplers," Appl. Phys. Lett. vol. 72, pp. 2637-8, May 1998.

12. Tada, K.; Hirose, K., “A new light modulator using perturbation of synchronism between two coupled guides,” (6th Conference on Solid State Devices, Tokyo, Japan, 2-3 Sept. 1974). Oyo Buturi, 1975, vol.44, suppl.: 61-6.
13. Cada, M.; Keyworth, B.P.; Glinski, J.M.; Rolland, C.; and others, “Electro-optical switching in a GaAs multiple quantum well directional coupler,” Applied Physics Letters, 19 June 1989, vol.54, (no.25): 2509-11.
14. Cavailles, J.A.; Erman, M.; Woodbridge, K., “Experimental study of switching in a p-i(MQW)-n vertical coupler,” IEEE Photonics Technology Letters, Nov. 1989, vol.1, (no.11):373-5.
15. Kohtoku, M., S. Baba, S. Arai and Y. Suematsu, "Switching operation in a GaInAs-InP MQW integrated twin guide (ITG) optical switch," IEEE Photon. Technol. Lett., vol. 3, pp. 225-6, Mar. 1991.
16. Dollinger, F., M. Borcke, G. Bohm, G. Trankle and G. Weimann, "Ultrashort low-loss optical multiquantum well GaAs/GaAlAs vertical directional coupler switch," Electro. Lett. vol. 32, 1509-10, Aug. 1996.
17. Boche, B.; Muller, R.; Bohm, G.; Trankle, G.; and others, “Monolithic integration of GaAs-AlGaAs quantum-well lasers with directional couplers using vertical coupling of light,” IEEE Photon. Technol. Lett., vol.8, pp.1591-3, Dec. 1996,.
18. Ikuta, S.; Kubota, S.; Pan, W.; Chu, S.T.; and others, “Stacked ARROW vertical coupler with large tolerance and short coupling length for three-dimensional interconnects,” Electro. Lett., vol.34, pp.1851-2, Sept. 1998.
19. Zucker, J. E., K. L. Jones, M. G. Young, B. I. Miller, and U. Koren, "Compact directional coupler switches using quantum well electrorefraction," Appl. Phys. Lett. vol. 55, pp. 2280-2, Nov. 1989.
20. Noda, S., N. Yamamoto and A. Sasaki, "New realization method for three-dimensional photonic crystal in optical wavelength region ," Japan. J. Appl. Phys. vol. 35, pp. L909-12, July 1996.
21. BeamProp, Version 2.0, Rsoft Inc. 1996.
22. Kuo-Liang Chen; Shyh Wang, “Cross-talk problems in optical directional couplers,” Applied Physics Letters, 15 Jan. 1984, vol.44, (no.2):166-8.
23. Chuang, S., “A coupled mode formulation by reciprocity and a variational principle,” Journal of Lightwave Technology, Jan. 1987, vol.LT-5, (no.1):5-15.
24. Chuang, S., “A coupled-mode theory for multiwaveguide systems satisfying the reciprocity theorem and power conservation,” Journal of Lightwave Technology, Jan. 1987, vol. LT-5, (no.1):174-83.
25. Chuang, S.-L., “Application of the strongly coupled-mode theory to integrated optical Devices,” IEEE Journal of Quantum Electronics, May 1987, vol.QE-23, (no.5):499-509.
26. Haus, H.A.; Huang, W., “Coupled-mode theory,” Proceedings of the IEEE, Oct. 1991, vol.79, (no.10): 1505-18.
27. Wei-Ping Huang, “Coupled-mode theory for optical waveguides: an overview,” Journal of the Optical Society of America A (Optics and Image Science), March 1994, vol.11, (no.3): 963-83.
28. Kim, B. -G., A. Shakouri, B. Liu, and J. E. Bowers, "Improved extinction ratio in ultra short directional couplers using asymmetric structures," Presented at the Integrated Photonics Research Conference, Vancouver, Canada, April 1998.
29. Kim, B. -G., A. Shakouri, B. Liu, and J. E. Bowers, “Improved extinction ratio in ultra short directional couplers using asymmetric structures,” Japanese Journal of Applied Physics, Part 2 (Letters), 1 Aug. 1998, vol.37, (no.8A): L930-2.

30. Haus, H.A.; Whitaker, N.A., Jr., “Elimination of cross talk in optical directional couplers,” Applied Physics Letters, 1 Jan. 1985, vol.46, (no.1): 1-3.
31. Liu, B., A. Shakouri, P. Abraham, Y. J. Chiu, S. Zhang, and J. E. Bowers, "InP/GaAs fused vertical coupler filter," accepted for publication IEEE Photon. Technol. Lett.
32. Liu, B., A. Shakouri, P. Abraham, and J. E. Bowers, "Fused vertical coupler switches," accepted for publication Electronics Letters
33. Shakouri, A., B. Liu, B. -G. Kim, P. Abraham, A. W. Jackson, A. Gossard, and J. E. Bowers, “Wafer fused optoelectronics for switching,” accepted for publication in Journal of Lightwave Technology.
34. Bandyopadhyay, A.; Basu, P.K., “Low-voltage vertical directional coupler switch with suppressed Electroabsorption,” IEEE Journal of Quantum Electronics, June 1996, vol.32, (no.6):1048-53.
35. Alferness, R. C., and R. V. Schmidt, “Tunable optical wavelength directional coupler filter”, Appl. Phys. Lett. 33(2), pp161-163, 1978.
36. Alferness, R. C., L. L. Buhl, U. Koren, M. G. Young, T. L. Koch, C. A. Burrus, and G. Raybon, “Broadly tunable InGaAsP/InP buried rib waveguide vertical coupler filter,” 1992, **60**, (8), Appl. Phys. Lett., pp. 980-982.
37. Chi Wu, C. Rolland, N. Puetz, R. Bruce, K. D. Chik, and J. M. Xu, “A vertically coupled InGaAsP/InP directional coupler filter of ultranarrow bandwidth,” 1991, **3**, (6), IEEE Photon. Technol. Lett., pp519-521.
38. Chi Wu, C. Rolland, F. Shepherd, C. Larocque, N. Puetz, K. D. Chik, and J. M. Xu, “InGaAsP/InP vertical directional coupler filter with optimally designed wavelength tunability”, IEEE Photon. Technol. Lett. 4(4), pp457-459, 1993.
39. Dug-Bong Kim; Chan-Yong Park; Beom-Hoan O; Hong-Man Kim; and others., “Fabrication of sidelobe-suppressed InP-InGaAsP vertical coupler optical filter using pair grating structure,” IEEE Photonics Technology Letters, Nov. 1998, vol.10, (no.11):1593-5.
40. Chu, S.T.; Miura, M.; Kokubun, Y., “Compact ARROW-type vertical coupler filter,” IEEE Photonics Technology Letters, Nov. 1996, vol.8, (no.11):1492-4.
41. Gehler, J.; Sato, S.; Sai Tak Chu; Wugen Pan; and others, “Narrowband optical wavelength comb by ARROW-type vertical coupler with thick cavity,” Electronics Letters, 6 Nov. 1997, vol.33, (no.23):1947-8.
42. Chu, S.T.; Pan, W.; Sato, S.; Maeda, T.; and others., “Sidelobe suppression of vertical coupler filter with an X-crossing Configuration,” Japanese Journal of Applied Physics, Part 1 (Regular Papers, Short Notes & Review Papers), June 1998, vol.37, (no.6B):3708-10
43. Pan, W.; Chu, S.T.; Sato, S.; Maeda, T.; and others., “Planarization of film deposition and improvement of channel structure for fabrication of anti-resonant reflecting optical waveguide type X-crossing vertical coupler filter,” Japanese Journal of Applied Physics, Part 1 (Regular Papers, Short Notes & Review Papers), June 1998, vol.37, (no.6B):3713-17
44. Miura, M.; Sai Tak Chu; Kaneko, T.; Kokubun, Y., “Design of X-crossing ARROW-type vertical coupler filter for narrow bandwidth and sidelobe reduction,” IN: Proceedings of OECC '97 2nd Optoelectronics and Communications Conference, Seoul, South Korea, 8-11 July 1997). Seoul, South Korea, p. 648-9.
45. Sang-Kook Han, “Side-lobe reduced vertical coupler wavelength filters,” IN: Proceedings of OECC '97 2nd Optoelectronics and Communications Conference, Seoul, South Korea, 8-11 July 1997). Seoul, South Korea, p. 266-7.

46. Han, S.-K.; Ramaswamy, R.V.; Tavlykaev, R.F., “Highly asymmetrical vertical coupler wavelength filter in InGaAlAs/InP,” Electronics Letters, 5 Jan. 1995, vol.31, (no.1):29-30.
47. Deri, R. J., M. A. Emanuel, F. G. Patterson, S. P. Dijaili, and L. T. Naguyen, “Polarization-insensitive wavelength filters by birefringence compensation of vertical couplers”, Appl. Phys. Lett. 68(8), pp1037-1039, 1996.
48. “Properties of Indium Phosphide”, emis DATAREVIEWS SERIES No.6, INSPEC, pp422-427, 1991.
49. “Properties of Aluminum Gallium Arsenide”, Edited by Sadao Adachi, emis DATAREVIEWS SERIES No. 7, INSPEC, pp126-140, 1993.